A MODIFIED TURBULENT KINETIC ENERGY MODEL FOR SWIRLING FLOW

A.A.A. Moustafa
Department of Engineering Math. and Phys., Faculty of Engineering,
Alexandria University, Alexandria, Egypt.

ABSTRACT

Flows with appreciable swirl occur in many engineering applications. The modelling of swirl flows using the standard two-equations k,ε model has been reported to have certain limitations, that restricts its application in its standard form [1,2]. A modified two-equations turbulence model based on the turbulent kinetic energy is applied to validate and develop computer codes for mathematical simulation of practical problems having swirling flow. The model properly includes corrections,such as "Richardson number" type for streamline curvature modifications, source-term in the dissipation energy equation and eddy viscosity formulation. This brings about significant improvements in the recirculation zone as well as the recovery region as compared with the experimental data. Two different types of swirl flow were examined to test the capability of the modified model, namely, the forced vortex and the jet swirl flow field.

1. INTRODUCTION

The generation of swirl in a flowing medium is simply by introducing a tangential or azimuthal velocity component to the medium. Various modes of generation have been utilized to accomplish this task; guide vanes, tangential entry swirl, rotating honeycomb or thick perforated disc, high speed rotation of a pipe [3] and complex multi-annular swiller [4]. Obviously, several structural or geometrical perturbations may exist for each mode of swirl generation with their accompanying disparities in efficiencies and resultant velocity profiles.

The standard form of the two equations turbulence models such as k,ε model are based on a homogeneous eddy viscosity distribution, which gives an isotropic turbulence generation. In flows with swirl, however, and indeed in 3D flows generally, the distribution of the flow field can be predicted using a different level of viscosity for each active stress component. Such an attempt is described in detail by [5]. So as the nonisotropic effects are predominant as in coaxial flows and flows through perforated plate, it is reported by [6,7] that the form of the turbulent distribution and eddy viscosity are functions of the characteristic flow parameters. The researchers of turbulence modelling have insisted that, their models describe properly the decay of turbulence in shear flows by using a transport terms [8].

Swirling flows are commonly used for creating strong and stable recirculating zones in gas turbine combustors and various types of burners.The Complexity of the strong swirling flow field requires careful consideration of turbulence model derivation and development. Subsequent discussion will focus on alternative modifications that may potentially enhance predictive accuracy.

The present work is carried out in order to systematically assess the applicability of the modified two-equations k-ε turbulence model to meaningful predictions of swirling flows.

Two cases were considered in order to investigate the swirling flow field namely, lateral jet-to- crossflow and the forced vortex flow in a pipe. The numerical study is based on the time-averaged finite volume form of the governing equations used as a tool to achieve the steady state solution.

Predicted and measured velocity profiles are compared, the comparison exhibit good agreement for the low swirl level, while the agreement deteriorates for the high swirl level.

2. MATHEMATICAL FORMULATION

The present work utilizes the "Semi-Implicit-Method for Pressure-Link equations" SIMPL Procedure outlined by Patanker [9]. The major advantages of this scheme over the traditional 'vorticity-stream function' formulations are the use of primitive variables, i.e velocity components and pressure, and its ready extension to three-dimensional recirculating flows. An overview of the governing time-averaged transport equations and the solution procedure is presented. A summary of the k-ε turbulence model and its modifications proposed for swirling flows is also discussed.

2.1. *The Governing Equations*

The motion of an incompressible swirling fluid is governed by a system of coupled nonlinear partial differential equations which are known as the Navier-Stokes-Equations "NSE". The general elliptic form of these equations in the three-dimensional cylindrical coordinates can by written [10] as:

$$\frac{1}{r}\frac{\partial}{\partial r}(\rho r u\phi)+\frac{1}{r}\frac{\partial}{\partial \theta}(\rho w\phi)+\frac{\partial}{\partial z}(\rho v\phi)$$

$$=\frac{1}{r}\frac{\partial}{\partial r}\left(r\Gamma_\phi\frac{\partial \phi}{\partial r}\right)+\frac{1}{r}\frac{\partial}{\partial \theta}\left(\Gamma_\phi\frac{1}{r}\frac{\partial \phi}{\partial \theta}\right)+\frac{\partial}{\partial z}\left(\Gamma_\phi\frac{\partial \phi}{\partial z}\right)+S_\phi$$

Where:

r,θ,z	are the radial, tangential and axial coordinate
u,v,w	are the time-averaged velocities in the radial, axial and tangential directions respectively.
ρ	is the fluid density
ϕ	stand for a general fluid property
Γ_ϕ	is the effective exchange coefficient of ϕ
S_ϕ	is the source term, contains quantities related to the generation or destruction of ϕ.

From the above general form, the governing equations of the flow can be obtained by suitable choosing for the exchange coefficient, Γ_ϕ and the source term S_ϕ. This leads to:

a) The continuity equation

It is obtained by setting:

$$\phi = 1\ ,\Gamma_\phi = 0 \text{ and } S_\phi = 0$$

b) The radial momentum equation

In this case;

$$\phi = u\ ,\ \Gamma_\phi = \mu_{eff} \text{ and}$$

$$S_u=\frac{\rho w^2}{r}-\frac{\partial p}{\partial r}+\frac{1}{r}\frac{\partial}{\partial r}\left(r\mu_{eff}\frac{\partial u}{\partial r}\right)+\frac{1}{r}\frac{\partial}{\partial \theta}\left(r\mu_{eff}\frac{\partial (w/r)}{\partial r}\right)$$

$$-2\frac{\mu_{eff}}{r}\left(\frac{1}{r}\frac{\partial w}{\partial \theta}+\frac{u}{r}\right)+\frac{\partial}{\partial z}\left(\mu_{eff}\frac{\partial v}{\partial r}\right)$$

where:

μ_{eff} is the effective viscosity coefficient given by $\mu_{eff} = \mu + \mu_t$, as μ is the physical viscosity of the fluid and μ_t is the turbulent viscosity which related to the turbulence energy k and its dissipation rate ε by ($\mu_t = \rho C_\mu k^2/\varepsilon$). Both k and ε being obtained from the solution of theirs respective transport equations. However the coefficient C_μ will be discussed in subsection 2.2.2.
p is the pressure.

c) The axial momentum equation

For this case the corresponding values of the coefficients are:

$$\phi = v\ ,\ \Gamma_\phi = \mu_{eff} \text{ and}$$

$$S_v=-\frac{\partial p}{\partial z}+\frac{1}{r}\frac{\partial}{\partial r}\left(r\mu_{eff}\frac{\partial u}{\partial z}\right)+\frac{1}{r}\frac{\partial}{\partial \theta}\left(\mu_{eff}\frac{\partial w}{\partial z}\right)+\frac{\partial}{\partial z}\left(\mu_{eff}\frac{\partial v}{\partial z}\right)$$

d) The tangential momentum equation

The coefficients takes the values:

$$\phi = w\ ,\ \Gamma_\phi = \mu_{eff} \text{ and}$$

$$S_w = \frac{-\rho v w}{r} - \frac{1}{r}\frac{\partial p}{\partial \theta} + \frac{1}{r}\frac{\partial}{\partial r}\left[r\mu_{eff}\left(\frac{1}{r}\frac{\partial u}{\partial \theta} - \frac{w}{r} \right) \right] + \frac{\mu_{eff}}{r}\left[r\frac{\partial (w/r)}{\partial r} + \frac{1}{r}\frac{\partial u}{\partial \theta} \right]$$
$$+ \frac{1}{r}\frac{\partial}{\partial \theta}\left[\mu_{eff}\left(\frac{1}{r}\frac{\partial w}{\partial \theta} + \frac{2u}{r} \right) \right] + \frac{\partial}{\partial z}\left[\mu_{eff}\frac{1}{r}\frac{\partial v}{\partial \theta} \right]$$

e) The turbulent kinetic energy equation

The transport equation for the kinetic energy of turbulent can be determined by setting the following values for the coefficients;

$$\phi = k\,,\ \Gamma_\phi = \mu_{eff}/\sigma_k \text{ and}$$

$$S_k = \mu_{eff}\left[2\left(\frac{\partial v}{\partial z}\right)^2 + 2\left(\frac{\partial u}{\partial r}\right)^2 + 2\left(\frac{1}{r}\frac{\partial w}{\partial \theta} + \frac{u}{r}\right)^2 \right.$$
$$\left. + \left(\frac{\partial v}{\partial r} + \frac{\partial u}{\partial z}\right)^2 + \left(\frac{\partial w}{\partial z} + \frac{1}{r}\frac{\partial v}{\partial \theta}\right)^2 + \left(\frac{1}{r}\frac{\partial u}{\partial \theta} + \frac{\partial w}{\partial r} - \frac{w}{r}\right)^2 \right] - \rho\varepsilon$$

with σ_k is the effective Schmidt number, its value for this case equal to one [11].

f) The turbulence dissipation rate equation

The transport equation for the dissipation rate of turbulent energy is obtained by the following coefficient values:

$$\phi = \varepsilon\,,\ \Gamma_\phi = \mu_{eff}/\sigma_\varepsilon$$

with the recommended value of 1.3 for the constant σ_ε [11].

The source term S_ε of the turbulent dissipation equation will be discussed in subsection 2.2.1.

2.2. *Turbulent Model Modification*

Turbulence computations are needed for practical simulations. Some success has been achieved with the standard k,ε model for relatively simple phenomena [12-17]. Failures are still common for many applications particularly those that involve strong curvature, intermittency, strong swirl and kinetically influenced chemical reaction [18].

The complexity of swirling flow fields requires careful consideration of turbulence model. The complex feature of the streamline charactesing the swirl flow field exerts a large influence on the turbulence structure of the flow. Curvature of streamlines affects primarily the higher-order correlations such as the turbulent stresses; the effect on viscous stresses is relatively negligible [19]. Consequently, the k-ε model has been subjected to a number of semi-empirical modifications in an effort to enhance its responsiveness to streamline curvature. such modifications may take at least two forms; the first is the source-term corrections in the k-ε standard form, particularly the dissipation equation. While the second is the corrections to the eddy viscosity itself by expressing the C_μ coefficient as a function of streamline curvature.

2.2.1. Source-term modification

In many flows, the stress field is generated by mean rates of strain in a plane orthogonal to it . This cross-planer influence gives rise to turbulence- driven "secondary motions", which are at variance with the conventional coincidence of the stress and strain axes and cannot be predicted by the standard form of k-ε model [20]. While secondary motion may have an important effects on some flows, it is questionable whether differences in the locations at zero shear stresses and zero mean velocity gradients are

computational significant in strong recirculating systems.

The dissipation rate equation is certainly responsible for a portion of the deficiency for swirling flows. The dissipation source-term control, to a significant degree, the magnitude of turbulent kinetic energy, the mean velocity decay, and the spreading rates. Dissipation source-term modifications generally adopt the guise of Richardson Number (which expresses the ratio of an apparent body force acting on a fluctuating or displaced fluid element, to a typical inertial force [19]). The Richardson number commensurate with turbulent systems can be written in the form of turbulent-time scale as [21].

$$R_i = \frac{k^2}{\varepsilon^2} \frac{U_s}{R_c^2} \frac{\partial (U_s R_c)}{\partial R_c}$$

where,

U_s is the velocity in the streamwise direction

R_c is the local radius of curvature of the streamline [22]

The Richardson number has not been optimized for swirling flows in general, and unfortunately, may be case-dependent. As is typical of the linear Richardson number relationships, an excessively large curvature correction or coefficient will force the dissipation source-term to adopt an unrealized sign change. Rodi [23] display this sensitivity to streamwise curvature as

$$S_\varepsilon = C_{\varepsilon 1} G \left(\frac{\varepsilon}{k}\right) - C_{\varepsilon 2}(1 - C_{gs} R_i) \frac{\rho \varepsilon^2}{k}$$

with

$$G = \mu_{eff} \left[2\left(\frac{\partial v}{\partial z}\right)^2 + 2\left(\frac{\partial u}{\partial r}\right)^2 + 2\left(\frac{1}{r}\frac{\partial w}{\partial \theta} + \frac{u}{r}\right)^2 + \left(\frac{\partial v}{\partial r} + \frac{\partial u}{\partial z}\right)^2 + \left(\frac{\partial w}{\partial z} + \frac{1}{r}\frac{\partial v}{\partial \theta}\right)^2 + \left(\frac{1}{r}\frac{\partial u}{\partial \theta} + \frac{\partial w}{\partial r} - \frac{w}{r}\right)^2 \right]$$

where the constant C_{gs} is assigned a value of 0.2 [22]. $C_{\varepsilon 1}$ and $C_{\varepsilon 2}$ are empirical constants having the values of 1.44 and 1.92 respectively [11].

2.2.2. *Eddy Viscosity Correction*

The purpose of the C_μ coefficient was to inquire whether a modification which affected the eddy viscosity directly, could achieve recirculation zone formation more rapidly (in a shorter axial distance), than the sluggish responsiveness associated with the dissipation source term corrections. As the effect of C_μ which produces a slight laminarization effect, the modified C_μ helps some what to promote a recirculation zone near the axis, relative to the k-ε model. Ultimately, such modification serves to prevent the tangential velocity from decaying as rapidly.

The dissipation source-term modifications may tend to respond more slowly to the flow field [23]. In addition, the Richardson number type corrections are largely empirical with a very limited applicability. For these reasons, attempts have been made to extract a C_μ coefficient from an algebraic formulation. The resultant functional form of the C_μ coefficient [22] is expressed as

$$C_\mu = \frac{0.09}{1 + 8k_1^2 \left(\frac{k}{\varepsilon}\right)^2 \left(\frac{\partial U_s}{\partial n} + \frac{U_s}{R_c}\right) \frac{U_s}{R_c}}$$

where k_1 is approximately equal 0.27 [11].

n is the outward normal unit vector to the streamline.

To preserve physical realism, C_μ is arbitrarily limited and allowed to range between 0.025 and 0.09 [11]. This corresponds to a decrease in the eddy viscosity and produces a slight laminarization that helps somewhat to promote a recirculation zone near the axis and serves ultimately to prevent the tangential velocities from rapidly decaying.

2.3. *Solution Procedure and Computer Requirement*

In order to solve the set of equations over the problem domain, the space is discretised into finite intervals or control volumes. The grid and the control volume in r-θ plane are shown in Figure (1). The finite domain equations are obtained by integrating the differential equations over the control volume cells. A hybrid difference scheme which combines the central and upwind difference approaches was used. Following the procedure of [24], we obtain the discretization equation has the form:

$$a_c \phi_c = a_E \phi_E + a_W \phi_W + a_N \phi_N + a_S \phi_S + a_T \phi_T + a_B \phi_B + b$$

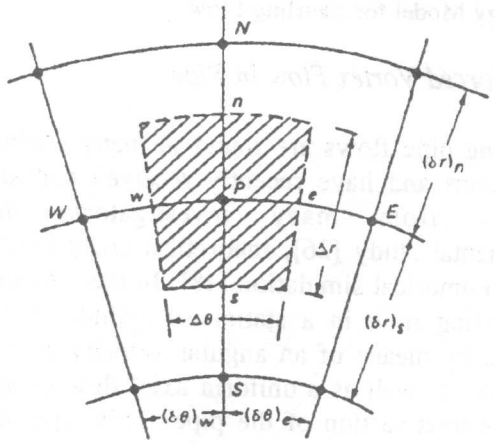

Figure 1. Control volume in cylindrical polar coordinates.

The subscript c refer to the center node of the control volume cell, while the subscripts E,W,N,S,T and B refers to east, west, north, south, top and bottom faces of that cell respectively.

The a's are coefficients which contain contributions from convection and diffusion terms, take the form:

$$a_I = D_i A(|h_i|) + [\![F_i, 0]\!]$$

where:

- I takes the meaning of E,W,N,S,T and B cell faces
- i takes the meaning of e,w,n,s,t and b the center of corresponding cell faces.
- D is the diffusion conductance
- F indicate the strength of the convection (flow rate), F can be take either positive or negative values depending on the flow direction.
- h is the Peclet number, defined as the ratio $(F/D)_i$.

The function $A(|h_i|)$ is taken corresponding to the scheme used (10) as listed below:

Scheme	Formula for $A(\|h_i\|)$
Central difference	$1- 0.5\|h_i\|$
Upwind	1
Hybrid	$[\![0, 1 -0.5 \|h_i\|]\!]$
Power law	$[\![0, (1-0.1 \|h_i\|^5]\!]$
Exponential (exact)	$\|h_i\| / [\![\exp \|h_i\| -1]\!]$

The symbol $[\![,]\!]$, stands for the largest of the quantities contained within it. While:

$$b = S_c \Delta V + \rho_c \Delta V/(\text{time step})$$

$$a_c = \sum a_I + a_{co} - S_p \Delta V$$

where,

- a_{co} is the coefficient of the initial value of any variable at the cell node divided by the time step.
- ΔV cell volume $= r\Delta r\Delta\theta\Delta z$
- S_p, S_c arise from the source term linearization [10].

The flow rates and the conductances are defined as:

$$F_e = (\rho u)_e \, \Delta r \Delta z \quad , \quad D_e = \frac{\Gamma_e \, \Delta r \Delta z}{(r\delta\theta)_e}$$

$$F_w = (\rho u)_w \, \Delta r \Delta z \quad , \quad D_w = \frac{\Gamma_w \, \Delta r \Delta z}{(r\delta\theta)_w}$$

$$F_n = (\rho v)_n \, r\Delta\theta\Delta z \quad , \quad D_n = \frac{\Gamma_n \, r\Delta\theta\Delta z}{(\delta r)_n}$$

$$F_s = (\rho v)_s \, r\Delta\theta\Delta z \quad , \quad D_s = \frac{\Gamma_s \, r\Delta\theta\Delta z}{(\delta r)_s}$$

$$F_t = (\rho w)_t \, r\Delta r\Delta\theta \quad , \quad D_t = \frac{\Gamma_t \, r\Delta r\Delta\theta}{(\delta z)_t}$$

$$F_b = (\rho w)_b \, r\Delta r\Delta\theta \quad , \quad D_b = \frac{\Gamma_b \, r\Delta r\Delta\theta}{(\delta z)_b}$$

As Γ_i is the diffusion flux and its value is obtained by the prescription presented in [10].

The slab by slab method is used to obtain converged solution iterativelly. For each calculation cycle, the three components of velocity (initial guesses), k and ε at all internal points are computed from the respective transport equations. The cell pressure and velocities are then adjusted iterativelly to satisfy the continuity equation.

Because of the nonlinearities of the partial differential equations and the strong interlinkage between them, numerical instability may develop leading to divergence in the solution procedure. For this reason, underrelaxation factors were used to promote stability. These factors were 0.3 for the velocity components and 0.8 for k, ε equations. The turbulent viscosity field was also underrelaxed with a value of 0.2. No relaxation was applied to the pressure correction field. The iterations were terminated when the sum of the absolute residuals (normalized, e.g., by the inlet mass flow rate, etc.) was less than 10^{-5}.

The number of iterations needed was of order 2000. The calculations were carried out by the general

purpose computer package **PHOENICS** [25] (**P**arabolic,**H**yperbolic,**O**r **E**lliptic **N**umerical **I**ntegration **C**ode **S**eries), at the University of Strathcyled, Glasgow U.K. The CPU time, on VAX-E 8600, required for convergence criteria was 21550 Sec. for a solution domain of grid size 30x30x100 in r, θ and z directions respectively.

3. RESULTS AND DISCUSSION

Two cases of swirl flow applications were studied to examined the capabilities and limitations of the modified turbulence model. Since the standard k, ε model is inadequate for the simulation of such complex flow field as discuses above in section (2.2) so, the calculations were made using the modified model only. The following section presents the results for each case, with a brief note on its applications.

3.1. *Forced Vortex Flow in Pipe*

Swirling pipe flows are found in many engineering applications and have recently received considerable attention from many investigators, through experimental study [26], theoretical analysis [27], as well as numerical simulation [28]. In the present case, the swirling flow in a stationary cylindrical pipe is obtained by means of an angular velocity at the inlet boundary, as well as a uniform axial flow component over the inlet-section of the pipe. This type of swirl flow is governed by a strongly anisotropic nature, specially over the inlet zone, which need a special attention of handling the turbulent treatment. This case is carried out in order to justify the limitations of the considered modified turbulence model in developing such a complex swirl flow.

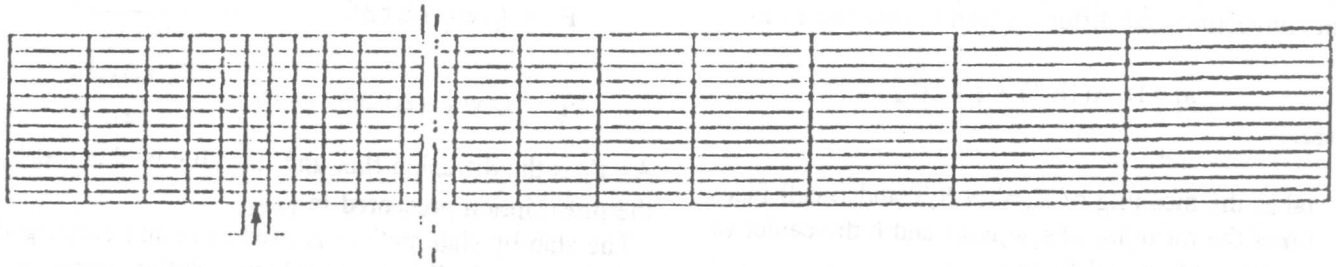

Fig. 2. Grid distribution in the rz plane showing the position of tangential intel velocity.

The general arrangement of the problem considered is shown in Figure (2). The boundary conditions governing the flow field were specified at the various planes. At the outlet boundary, the flow assumed to be fully-developed, i.e. the axial gradients of all variables are set to zero. On the symmetry axis (centerline), the radial velocity and the normal gradient of the other variables are set to zero. At the wall, the normal velocity is set to zero, while near-wall tangential velocities are connected with their zero wall values by way of the wall function, as outlined by Launder and Spalding [29]. For the inlet boundary, the computational details for predicting the flow fields corresponding to the experimental conditions of [26] were selected for verification purposes. For reasons of brevity, only the major features of the flow are presented at different sections along the axis of the pipe as given in the following table.

Section	a	b	c	d	e	f	g
z/d	70	60	50	42	34	13	5

Figure (3) illustrates the computed axial velocity profiles as compared with experimental profiles of [26]. Over the inlet region, where a swirl component is given to the flow, some kinds of unsteadiness and axi-asymmetry appear on the flow as already demonstrated by [26]. The strongly anisotropic nature of the flow in this region seems to be the reason of the sluggish behaviour of the predicted axial velocity components over this zone.

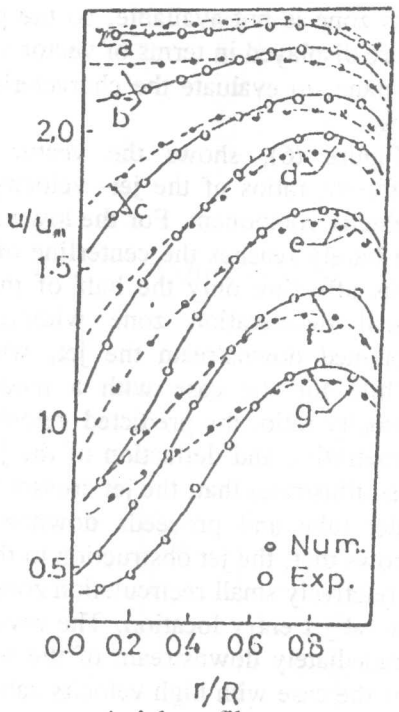

Axial profiles

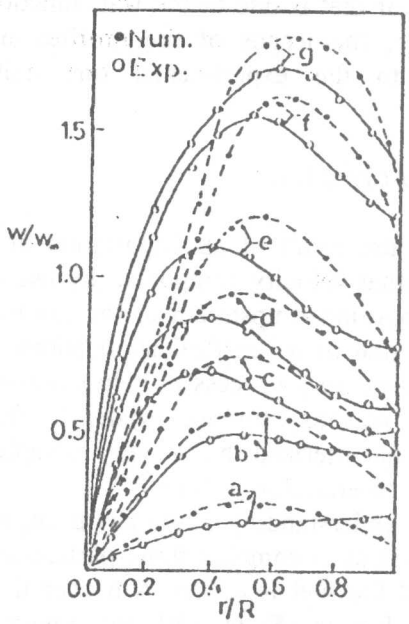

Tangential profiles

Figures 3,4. Axial and Tangential velocity profiles "The experimental profiles after [26]"

From a quantitative point of view, the following is noticed. Over the lateral region ($0<r/R<0.5$), the numerical results give overestimated values than the corresponding experimental ones. It was found that, the relative percentage difference defined by {(numerical value-experimental value)/experimental value}x100, this values are variant along the axial direction on the center of the chamber form 30% at the inlet section ($z/d=15$) to a value of 14% at the middle region ($z/d=50$). For the downstream regions ($z/d>60$) this values tenets to @4%. On the other hand, the overestimated values decreases in magnitude in the lateral direction for each section ($z/d=$constant), and approaches zero at the lateral section ($r/R=0.5$). Along the axial direction, of the centerline at ($r/R = 0.2$), the relative values are 20% at ($z/d=30$) and 4% at ($z/d=40$). However, over the lateral region ($0.5<r/R<1$), the numerical values gives underestimated flow field, specially near the wall. Also the values of these difference decreasing along the axial direction. From the figure, along the section $r/R=0.8$, the relative values are -7% at ($z/d=13$) and -3% at ($z/d=30$) (the negative singe indicate the underestimated values).

It is clear from the figure that when the swirl is sufficiently strong, i.e at the inlet zone, the numerical model is not accurate enough, while for the fully developed regions, the model gives a values in good agreement with the experimental profiles.

The tangential velocity profiles issuing from such swirl generators assume a combination of the forced and free vortex distributions. The mean tangential velocity in the flow field must go to zero at the axis of the symmetry and hence, solid-body rotation necessarily exists in the centerline region surround by an outer free vortex flow. Figure (4), shows again, the underestimated tangential velocity component obtained numerically over the central core region ($0<r/R<0.35$). The reason of this slow decaying for the forced vortex region is believed to the slow response of the modified model for the high stress zone. For the outer lateral domain ($0.35<r/R<1$), the numerical values give overestimated than the experimental ones within a relative percentage

difference of (12% at z/d=60 and r/R=0.6), this value tenets to zero along the section (r/R=0.8). Also near the wall, the numerical values again is underpredicted, usually, the reason of that is due to the wall function treatment. However, the trends of the profiles are predicted similar to the experimental one quite satisfactory.

3.2. *Lateral Jet-to-Crossflow*

Swirl jet flow is the result of an impartation of a tangential or azimuthal velocity component by use of a swirl generator positioned upstream of the reactor. Lateral jet flow is one of a practical applications to provide additional flow in a process to help complete mixing for special reasons "furnaces system". This type of flow is characterized by a very complex velocity field, with reverse flow nature.

To achieve better understanding of the key transport processes involved in such complex flow, particularly of burner swirl and the fuel injection. A burner flow case illustrated in Figure (5) is card out, under a conditions to suit the experimental data of [30,31]. The boundary conditions of the solution domain, were specified at different planes. At the out flow plane, zero normal gradient or continuation condition is imposed and the normal velocities are assigned to ensure macroscopic mass balance. On the wall, the will known wall function is applied for velocity treatment near the wall. For the inlet plane a uniform profile flow is taken over the cross section of the inlet tube, in addition to the lateral jet flow. The main objective of this case, is to developed the prediction of this type of flows, as well as to examined the capability of the proposed modifications for the turbulence model to suit such kind of flow phenomena.

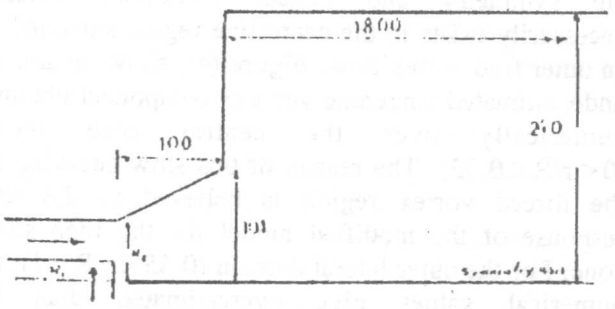

Figure 5. General arrangement for the burner case [30]

For the inlet region, where the lateral jet flow active with the axial flow field, the experimental results for this zone is not available, so the predicted flow field were displayed in terms of vector velocity pattern in r-z plane, to evaluate the characteristic feature of such flow.

Figure (6), shows the vector velocity field for different ratios of the jet- velocity to the main axial velocity component. For the low value ratio the lateral jet barely reaches the centerline of the inlet tube, and thus affecting only the half of the inlet cylinder. A small deceleration zone without reverse flow is obtained downstream the jet, which rapidly decay. While for the case with a moderate value of the velocity ratio, the predicted velocity vectors show the penetration and deflection of the jet flow. The figure also illustrates that, the jet crosses the centerline of the inlet tube and proceeds downstream . The pattern shows that, the jet obstruction to the crossflow created a relatively small recirculation zone downstream of the lateral jet entry location. The reverse flow is obvious immediately downstream of the jet plane. Moreover, for the case with high velocity ratio, the figure clearly shows that, the jet crosses the centerline of the inlet tube and almost reaches the opposite wall. A big recirculation zone is formed, with a height nearly three quarters of the inlet tube diameter. These features were observed in the flow visualization. It is obvious that, as the velocity of the lateral jet increases its radial penetration increases, as well as the size of the recirculation zone with a reverse flow zone downstream of the jet plane.

For the region inside the chamber, where the experimental data are available. Samples of the results are illustrated in the form of radial profiles of the axial and tangential velocity components, at different planes through the axis of the chamber. Two different levels of swirling number which characterizes the intensity of swirl are examined.

Figure (7) illustrates comparison of the predicted velocity map of the flow field and the experimental data [30,31], for two sample of flow settings with swirl numbers 0.45 and 2.225.

Axial velocity profiles are of principal importance, they illustrate the jet boundary, degree of expansion and regions of high velocity gradient. They also define the boundaries of the forward and reversed flow zones, the latter being fundamental to the mechanism of frances flame stabilization.

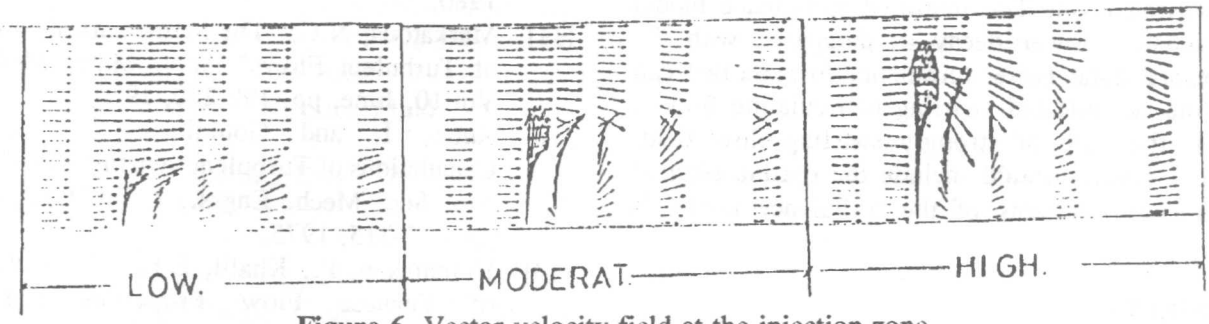

Figure 6. Vector velocity field at the injection zone

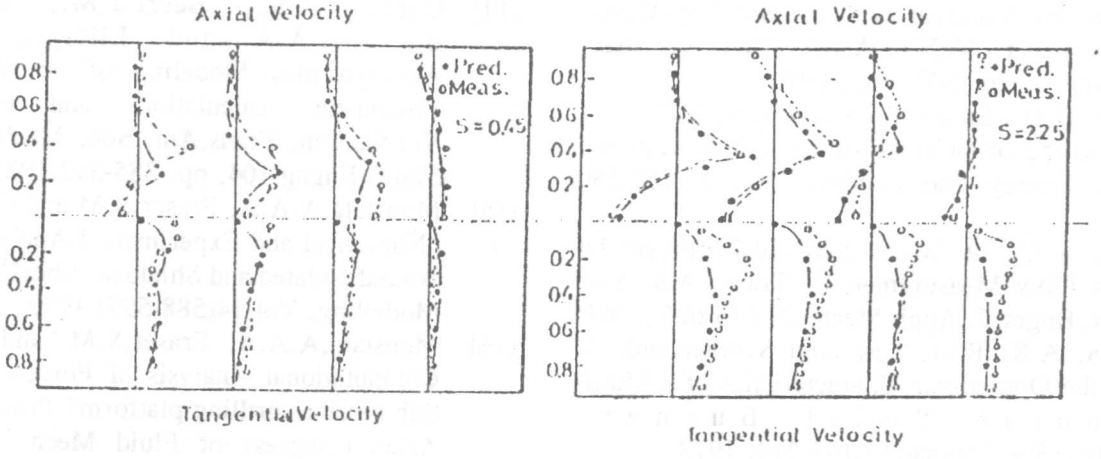

Figure 7. Comparison of axial and tangential profiles

The agreement between the predictions and experimental data was achieved, for the axial velocity profiles particularly in the outer flow region ($r/R > 0.5$). While for the central core region ($r/R < 0.5$) where the shear stress is predominant, the numerical values becomes underpredicting within a relative percentage difference of (20% near the inlet section and decreasing rapidly along the axial direction.

The main flow features such as forward flow in the outer part of the chamber with peak velocities increasing with increasing of the swirl level are well predicted . While, a negative axial velocity (reverse flow) in the central core of the chamber is predominated. These reverse flow may also extending over the entry region as the swirl level increase.

For the tangential velocity profiles, it is noticed that, the predicted values sees the usual Rankine type flow with solid body central rotation. The deflection outward is pronounced, the peak values of the tangential component increase and its location moved outward as the swirl is increased. The agreement with the experimental data is achieve over the lateral region ($0.4 < r/R < 1$) with a very small relative difference. While, over the central core region ($r/R < 0.4$), some relative difference were noticed, that varying from 25% for the high swirl level at the inlet section, to 10% for the low swirl level.

4. CONCLUSION

The developed predictions present a basic tool to show the influence of the turbulence model on handling swirling recirculating flow situation. Predicted results give important trends in the flow such as jet penetration, defection and swirling crossflow effects. Comparison with measured velocity profiles shows that the quality of the predicted results is good, however, the inaccuracies in some details occur specially with

high swirling level. The modified turbulence model accommodates slower decay as compared with the experimental data. Better turbulence formula that can handle the complicated swirling recirculating flow is need for the case of strongly swirling flow field. Additional studies would include the optimization of the empirical constants of the turbulence model is needed.

REFERENCES

[1] Abujelala, M.T. and Lilley,D.G. "Limitations and empirical extensions of the k-ε model as applied to turbulent confined swirling flows" AIAA paper 84-0041,AIAA 22nd Aerospace Meeting, Reno, NV, Jan., 1984.

[2] Sloan, D.G., Smith, P.J and Smoot, L.D. "Modelling of swirl in turbulent flow systems" Prog. Energy and combust. Sei.,12,163-250 1986

[3] Rose, W.G. "A Swirling Round Turbulent Jet Mean Flow Measurements", Trans. Am. Soc. Mech. Engrs. J. Appl. Mech. 29,615-625 (1962)

[4] Gupta, A.K. Beer, J.M. and Swithenbank, J. "On the Operational Characteristics of a Multi-annular Swirl Burner" Cambist,Sci,Technal,17,197-214, 1978.

[5] Launder,B.E "An improved algebraic stress model for turbulence" Imperial collage, Mech, Eng.Dept Rep TM/TN/A. 1971.

[6] Moustafa, A.A.A " Numerical and Experimental Investigation of the Aerodynamic action of perforated windbreak" Proc. of the Eighth International conference for Mechanical Eng.(249-261). Alexandria April, 1993.

[7] Moustafa A.A.A " Finite Element Simulation for Confined Mixing of Coaxial Flows"Proc. of the Eighth International conference for Mechanical Eng.(237-248). Alexandria April, 1993.

[8] Singh, S.N, Agrawal, D.P, Mathotra, R.C. and Raghava A.K. "velocity predictions of contra-swirling jets in a sudden expanding confinement" AIAA. J.25, 161-163 1987.

[9] Patanker,S.V. and Spalding, D.B "A calculation Procedure for heat, mass and momentum transfer in three-dimensional parabolic flows" Int.J. Heat and Mass Transfer 15, pp. 1787-1806, 1972.

[10] Patankar,S.V " Numerical Heat Transfer and Fluid Flow" Hemisphere publishing corporation 1980.

[11] Markatous, N.C," The Mathematical Modelling of Turbulent Flows" Appl. Math. Modelling, Vol 10, June, pp. 190-220, 1986.

[12] Kubo, I. and Gouldin, F.C "Numerical Calculations of Turbulent Swirling Flow" Trans, Am, Soc. Mech. Engrs., J. Fluid Engng. 97, pp. 311-315, 1975.

[13] Hutchinson, P., Khalil, E.E. "The Calculation of Furnace Flow Properties and their Experimental Verification" Trans. Am. Soc. Mech. Engrs. J. Heat Transfer 98, pp. 276-283 1976.

[14] Gupta, A.K., Beerr,J.M., Louis,J.F., Busnaina,A.A and Lilley,D.g "Flow Aerodynamics Modeling of an MHD Swirl Combustor: calculations and experimental Verification, Trans,Am. Soc. Mech. Engrs, J. Fluids Engng 104, pp. 385-392 1982.

[15] Moustafa,A.A.A, Fraser,S.M and Carey, C. "Numerical and Experimental Analysis of Flow around Isolated and Shielded cubes" App. Math. Modelling, Vol 14(588-597) 1990.

[16] Moustafa,A.A.A, Fraser,S.M. and Carey,C." Computational Analysis of Forces on a Semi-Submersible drilling platform" Proc. of the 4th Asian Congress of Fluid Mech. Hong-Konk 1989.

[17] Moustafa,A.A.A "modelling of Flow over Step with complex geometry using Multigrid system" Proc. of 23th ISCE symposium on stochastic systems,Theory and Application. OSAKA,JAPAN, Nov. 1991.

[18] Hoffman,N. and Markatos,N.C." Thermal radiation effects on fires in enclosure " Appl. Math. Modelling, Vol 12 April 129-140 1988.

[19] Bradshaw,P "The Analogy between Streamline Curvature and Buoyancy in Turbulent Shear Flow", J. Fluid, Mech, 36,177-191 (1969)

[20] Pope,S.B and Whitelaw,J.H "The Calculation of Near-Wake Flows" J.Fluid Mech. 73,9=32 (1976).

[21] Launder,B,E., Pridding,C.H. and Sharama,B.I. "The Calculation of Turbulent Boundary Layers on Spinning and Curved Surfaces", Trans. Am. Soc. Mech. Engrs, J. Fluid Engng. 99, 231-239 (1977).

[22] Leschziner,M.A and Rodi,W. "Calculation of Annular and Twin Parallel Jets Using Various Discretization Schemes and Turbulence Model

Variations" J. Fluid Engng 103, 352-360 (1981).

[23] Rodi, W. and Scheuerer,G. " Calculation of Curved Shear Layers with Two-equation Turbulence models," Physics Fluids 26,1422-1436 (1983).

[24] Rosten,H.I and Spalding,D.B " The PHOENICS Equations" CHAM TR/99 CHAM Limited ,Surry,London 1989.

[25] Spalding,D.B and Rosten,H.I " A Lecture course on PHOENICS Code system" CHAM Report UK/TR/101/2 1986.

[26] Murakami, M., Kito,O., Katayama,Y. and Iida, Y "An Experimental Study of Swirling Flow in Pipes" Bulletin of the JSME, Vol.19, pp 118-126 (1976)

[27] Kreith,F and Sonju,O.K. J. Fluid Mech., vol.22, part 2 ,p. 257 (1965).

[28] Rochino,A.P. and Lavan,Z., Trans. ASME. Ser.E vol. 36-2 P. 151 (1969)

[29] Launder,B.E. and Spalding, D.B " Numerical Computation of Turbulent Flows" Comp. Methods in Appl. Mech. and Engrg., vol 3, pp 269-289- (1974).

[30] Beltagui,S.A. and Maccallum, N.R.L. " Aerodynamic of Vane-swirl Flames in Furnaces " J.Inst. Fuel. vol,49,pp 183-193 (1976)

[31] Beltagui,S.A and Ralston, T., "An Isothermal Model Study of Aerodynamics and Mixing Burner, NEL Report, No. dc/370,East Kilbride, Glasgow: National Engineering Laboratory, 1984.